Eur. J. Mineral.
2016, **28**, 655–661
Published online 2 March 2016

Ferraioloite, $MgMn^{2+}_4(Fe^{2+}_{0.5}Al^{3+}_{0.5})_4Zn_4(PO_4)_8(OH)_4(H_2O)_{20}$, a new secondary phosphate mineral from the Foote mine, USA

STUART J. MILLS[1,*], IAN E. GREY[2], ANTHONY R. KAMPF[3], COLIN M. MACRAE[2], JASON B. SMITH[4], CAMERON J. DAVIDSON[2] and A. MATT GLENN[2]

[1] Geosciences, Museum Victoria, GPO Box 666, Melbourne 3001, Victoria, Australia
*Corresponding author, e-mail: smills@museum.vic.gov.au
[2] CSIRO Mineral Resources, Private Bag 10, Clayton South 3169, Victoria, Australia
[3] Mineral Sciences Department, Natural History Museum of Los Angeles County, 900 Exposition Boulevard, Los Angeles, CA 90007, USA
[4] 1304 Kennon St., Charlotte, NC 28205, USA

Abstract: Ferraioloite, $MgMn^{2+}_4(Fe^{2+}_{0.5}Al^{3+}_{0.5})_4Zn_4(PO_4)_8(OH)_4(H_2O)_{20}$, is a new secondary phosphate mineral from the Foote Lithium Company mine, Kings Mountain district, Cleveland County, North Carolina, USA. The mineral was found in tiny vughs within a thin seam of very fine-grained, sugary pegmatite with vivianite, fairfieldite/messelite, phosphophyllite, scholzite/parascholzite, rittmannite, mangangordonite, kingsmountite, kastningite and metaswitzerite. Ferraioloite crystals occur as very thin greenish grey to lemon yellow plates or blades up to about 0.2 mm in length, but no more than a few μm thick. Crystals are biaxial (−), with indices of refraction $\alpha = 1.575$(calc), $\beta = 1.5825(5)$, $\gamma = 1.5835(5)$, $2V$(meas.) = 40(5)°. Dispersion is weak: $r > v$, the orientation is: $X \approx \mathbf{a}$, $Y = \mathbf{b}$, $Z \approx \mathbf{c}$ and pleochroism: X, Z = colourless, Y = blue grey; $Y >> X \approx Z$. The empirical formula (based on 56 O atoms pfu) is $Ca_{0.21}Mg_{0.50}Mn^{2+}_{4.16}Fe^{2+}_{2.05}Al^{3+}_{2.01}Zn_{4.27}P_{8.00}H_{43.59}O_{56}$. Ferraioloite is monoclinic, space group $I2/m$, with the unit-cell parameters: $a = 25.333(3)$ Å, $b = 6.299(1)$ Å, $c = 15.161(3)$ Å, $\beta = 90.93(3)°$ and $V = 2419.0(2)$ Å^3. Ferraioloite has a heteropolyhedral layer structure with layers parallel to (100) and with isolated $Mg(H_2O)_6$ octahedra and water molecules packing between the layers. The heteropolyhedral slabs have the same topology as falsterite, with Mn^{2+} replacing Ca^{2+} and with Al^{3+} substituting for Fe^{3+}.

Key-words: ferraioloite; new mineral; falsterite; pegmatite; Foote Lithium Company mine; crystal structure; synchrotron; phosphate.

1. Introduction

The new mineral ferraioloite was discovered by one of the authors (JBS) in 2005 on the East dump of the Foote Lithium Company mine, Kings Mountain district, Cleveland County, North Carolina, USA (35°12'40''N, 81°21'20''W). The pegmatite exploited by the Foote Lithium Company mine is the type locality for twelve other minerals (*e.g.* White, 1981; Atencio *et al.*, 2008), seven of which are secondary phosphates.

The resemblance of the new phase to the recently described mineral falsterite (Kampf *et al.*, 2012) was noted early in our study; however, the very thin, curved nature of crystal plates presented challenges in its characterization, especially with respect to the determination of its crystal structure. Falsterite was described from the Palermo No. 1 pegmatite, North Groton, New Hampshire, USA, where it occurs in a secondary phosphate assemblage rather similar to that in which ferraioloite was discovered at the Foote mine. Falsterite has also been found at the Estes pegmatite quarry, Baldwin, Maine, USA. At both of these occurrences, falsterite is associated with schoonerite (Kampf, 1977; Moore & Kampf, 1977), a mineral with which it has structural affinities. Interestingly, schoonerite has also been found in the same general assemblage as ferraioloite at the Foote mine. Considering that schoonerite is known from several other pegmatites, including the Hagendorf Süd pegmatite, Bavaria, Germany, it is reasonable to expect ferraioloite to be found in other phosphate-bearing pegmatites in the future.

The species is named in honour of the late James (Jim) Anthony Ferraiolo (May 14, 1947−February 6, 2014). The mineral is pronounced /fe..(r) i: 'Ou lOu ait/ (/feə- i: 'o- lo- a-t/). Jim worked as scientific assistant at the American Museum of Natural History (AMNH) from April 1978 until August 1982 and also as transaction coordinator at the Smithsonian Institution's Museum of Natural History from September 1982 until April 1985. He was best known for his publication *A Systematic Classification of Nonsilicate Minerals* (Bulletin 172 of the AMNH, 1982),

DOI: 10.1127/ejm/2016/0028-2525
0935-1221/16/0028-2525 $ 3.15

which was widely used in Museum collections, as a basis for collection classification and organisation (*e.g*. Museum Victoria, Australia). Recently, Jim was a member of the IMA CNMNC subcommittee for mineral group nomenclature and the subcommittee on unnamed minerals. Jim also spent more than a decade as a manager with mindat.org and was instrumental in publishing the description of ferrolaueite (Ferraiolo, 2012; Segeler *et al.*, 2012).

The mineral and name (IMA2015−066) were approved by the IMA CNMNC prior to publication. Two cotype specimens are housed in the collections of Museum Victoria, specimen M53492 and M53493, and two cotype specimens are deposited in the collections of the Natural History Museum of Los Angeles County, catalogue numbers 65593 and 65594.

2. Occurrence, location and physical and optical properties

The new mineral occurs in very small vughs contained in a thin seam of very fine-grained, sugary pegmatite (~30 × 10 × 20 cm) as a stringer in more typical pegmatite that was part of a large zinc-bearing boulder found on the East dump (the only zinc-bearing phosphates ever found at the locality were found in this boulder). Mn-bearing fluorapatite, sphalerite, muscovite and pyrite are common accessory minerals in the stringer as well as in other places in the larger boulder. Associated secondary minerals in order of abundance are: vivianite, fairfieldite/messelite (as boxwork-like networks forming cavity walls), phosphophyllite, scholzite/parascholzite, rittmannite, mangangordonite, kingsmountite, kastningite and, on two specimens, metaswitzerite.

Ferraioloite crystals occur as very thin greenish grey to lemon yellow plates or blades up to about 0.2 mm in length, but no more than a few μm thick (Fig. 1). Individual crystals may also show curved faces. The main faces observed are {010}, {100} and {011} (Fig. 2). The plates often form books or rosettes up to about 0.4 mm across. Crystals are transparent with a vitreous lustre, flexible with an irregular fracture, and have perfect cleavage on {100}. The Mohs' hardness is estimated to be about 2, based upon behaviour when broken.

The density could not be measured because insufficient material is available for direct measurement. The calculated density is 2.59 g cm^{-3}, based on the empirical formula and single-crystal unit cell. Optically, ferraioloite crystals are biaxial (−), with indices of refraction α = 1.575(calc), β = 1.5825(5), γ = 1.5835(5), $2V$(meas.) = 40(5)° and $2V$(calc.) = 40°, measured in white light. The thinness of the plates made it impossible to accurately measure α; consequently, it has been calculated based upon β, γ and $2V$. Dispersion is weak: $r > v$, the orientation is: $X \approx \mathbf{a}$, $Y = \mathbf{b}$, $Z \approx \mathbf{c}$ and pleochroism: X, Z = colourless, Y = blue grey; $Y >> X \approx Z$. The Gladstone−Dale compatibility is −0.0416 (good) using the empirical formula and single-crystal unit cell.

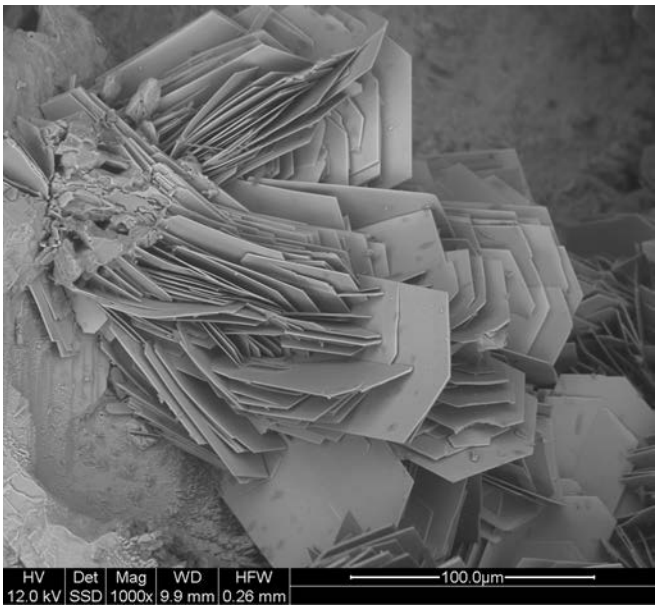

Fig. 1. Scanning electron microscope (SEM) image of intergrown blades of ferraioloite.

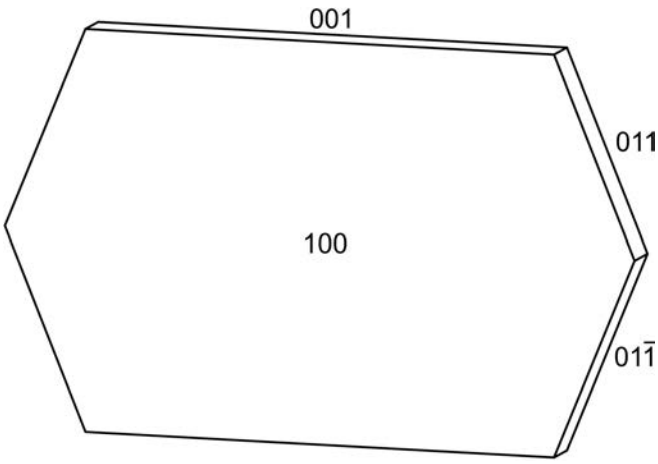

Fig. 2. Crystal drawing of a blade of ferraioloite.

3. Chemical composition

Quantitative chemical analyses (10) of ferraioloite were carried out using a wavelength dispersive spectrometer on a JEOL JXA 8500F Hyperprobe operated at an accelerating voltage of 12 kV and a beam current of 3 nA. The beam was defocused to 5 μm. Water could not be analysed directly because of the minute amount of sample available. H_2O was calculated on the basis of P = 8, charge balance and 56 O atoms per formula unit (*apfu*), as determined by the crystal-structure analysis (see below). Analytical data are given in Table 1.

The empirical formula of ferraioloite (based on 8 P and 56 O *apfu*) is $Ca_{0.21}Mg_{0.50}Mn^{2+}_{4.16}Fe^{2+}_{2.05}Al^{3+}_{2.01}Zn_{4.27}P_{8.00}H_{43.59}O_{56}$. The simplified formula is $MgMn^{2+}_{4}$

Table 1. Analytical results (wt.%) for ferraioloite.

Const.	Mean	Range	SD	Standard
CaO	0.65	0.51–0.75	0.09	wollastonite ($CaSiO_3$)
MgO	1.09	0.92–1.23	0.09	spinel ($MgAl_2O_4$)
MnO	16.05	14.2–19.51	1.36	rhodonite ($MnSiO_3$)
ZnO	18.90	16.76–20.15	1.07	phosphophyllite ($Zn_2(Fe,Mn)(PO_4)_2{\cdot}4H_2O$)
FeO	8.02	5.71–9.47	1.26	hematite (Fe_2O_3)
Al_2O_3	5.58	5.23–5.99	0.23	berlinite ($AlPO_4$)
P_2O_5	30.90	29.52–32.17	0.83	berlinite ($AlPO_4$)
H_2O*	21.30			
Total	102.49			

* Calculated from structure

$(Fe^{2+}_{0.5}Al^{3+}_{0.5})_4Zn_4(PO_4)_8(OH)_4(H_2O)_{20}$, which requires MgO 2.17, MnO 15.26, FeO 7.73, ZnO 17.52, Al_2O_3 5.48, P_2O_5 30.54, H_2O 21.30, total 100.00 wt.%.

4. Powder X-ray diffraction

Powder X-ray diffraction data for ferraioloite were obtained on a Rigaku R-Axis Rapid II curved–imaging–plate microdiffractometer utilising monochromatised Mo$K\alpha$ radiation. A Gandolfi-like motion on the φ and ω axes was used to randomize the sample. Observed d spacings and intensities were derived by profile fitting using JADE 2010 software (Materials Data Inc.). Data are given in Table 2. The unit-cell parameters refined from the powder data using JADE 2010 with whole-pattern fitting are: a = 25.320(6), b = 6.345(6), c = 15.267(6) Å, β = 91.031(5)°, V = 2452.4(4) Å^3 and Z = 2, which are in excellent agreement with the single-crystal study below.

5. Single-crystal X-ray diffraction

A pale green 20 μm × 10 μm × 2 μm lath of ferraioloite was mounted on a nylon loop, to minimise diffraction from the sample mount for an X-ray data collection on

Table 2. Powder X-ray data (d in Å) for ferraioloite (eight strongest lines in bold-face type).

I_{obs}	d_{obs}	d_{calc}	I_{calc}	hkl	I_{obs}	d_{obs}	d_{calc}	I_{calc}	hkl	I_{obs}	d_{obs}	d_{calc}	I_{calc}	hkl
		13.1016	2.5	$\bar{1}$ 0 1			2.8308	0.1	2 2 2			1.9574	0.2	$\bar{4}$ 1 7
		12.9155	2.4	1 0 1			2.8200	0.1	4 2 0			1.9365	0.1	$\overline{13}$ 0 1
100	**12.7**	12.6648	100.0	2 0 0			2.7882	0.1	$\bar{8}$ 1 1			1.9335	0.2	$\bar{8}$ 2 4
1	7.58	7.5795	0.9	0 0 2			2.7737	0.2	8 1 1			1.9184	0.1	$\bar{2}$ 3 3
		6.1128	0.2	1 1 0	**4**	**2.664**	2.6604	0.4	$\bar{1}$ 2 3	2	1.8942	1.9160	0.4	$\overline{10}$ 2 2
		5.8168	0.2	0 1 1			2.6557	0.4	1 2 3			1.9143	0.3	8 2 4
		5.2735	0.5	2 1 1			2.6492	1.0	$\bar{4}$ 2 2			1.9043	0.5	10 2 2
1	4.95	4.9709	0.5	$\bar{1}$ 0 3	3	2.616	2.6379	1.6	$\bar{5}$ 2 1			1.8949	1.0	0 0 8
		4.9400	0.4	1 0 3			2.6302	1.5	5 2 1			1.8797	0.3	$\bar{7}$ 2 5
4	**4.78**	4.8284	0.3	$\bar{5}$ 0 1			2.6203	0.6	$\bar{5}$ 0 5			1.8785	0.2	$\bar{2}$ 0 8
		4.7815	0.4	5 0 1	3	2.562	2.5831	0.7	5 0 5			1.8696	0.3	2 0 8
		4.7673	1.0	$\bar{1}$ 1 2			2.5545	0.9	$\bar{3}$ 2 3			1.8480	0.2	$\overline{11}$ 2 1
		4.7491	1.4	1 1 2			2.5419	0.5	3 2 3			1.8329	0.2	$\bar{1}$ 3 4
1	4.33	4.3672	0.4	$\bar{3}$ 0 3			2.5244	0.6	6 2 0			1.8308	0.2	1 3 4
		4.3052	0.7	3 0 3			2.4838	0.2	$\bar{8}$ 1 3			1.8196	0.1	11 0 5
4	**4.22**	4.2216	1.1	6 0 0	3	2.404	2.4222	0.2	0 2 4			1.8012	0.1	13 1 2
		4.1832	0.8	3 1 2			2.4020	1.0	$\bar{6}$ 2 2			1.7628	0.1	7 3 2
		3.7771	0.2	$\bar{2}$ 1 3			2.3907	0.2	10 0 2			1.7598	0.2	$\overline{10}$ 2 4
		3.7500	0.1	2 1 3			2.3881	1.3	6 2 2			1.7506	0.2	$\bar{3}$ 2 7
3	3.699	3.7138	1.2	$\bar{6}$ 0 2			2.3837	0.9	$\bar{2}$ 2 4			1.7416	0.3	10 2 4
		3.6629	1.3	6 0 2	2	2.352	2.3746	0.3	2 2 4			1.7134	0.1	$\overline{12}$ 2 2
		3.6470	0.6	$\bar{2}$ 0 4			2.3556	0.3	5 2 3			1.7033	0.1	12 2 2
4	**3.580**	3.6146	0.4	2 0 4			2.3427	0.4	$\bar{7}$ 0 5			1.6827	0.5	$\bar{8}$ 2 6
		3.6070	0.6	$\bar{5}$ 0 3			2.3382	0.1	$\bar{1}$ 1 6			1.6813	0.1	$\overline{15}$ 0 1
		3.5489	0.9	5 0 3			2.3317	0.3	1 1 6			1.6753	0.2	15 0 1
		3.5326	0.2	$\bar{7}$ 0 1			2.3276	0.3	$\overline{10}$ 1 1			1.6637	0.4	8 2 6
5	**3.499**	3.5195	3.2	$\bar{5}$ 1 2			2.3171	0.4	10 1 1			1.6431	0.2	$\overline{14}$ 0 4

(*Continued*)

Table 2. Continued

I_{obs}	d_{obs}	d_{calc}	I_{calc}	*hkl*	I_{obs}	d_{obs}	d_{calc}	I_{calc}	*hkl*	I_{obs}	d_{obs}	d_{calc}	I_{calc}	*hkl*
		3.5068	0.2	7 0 1			2.3056	0.2	7 0 5	2	1.6178	1.6237	0.2	0 2 8
		3.4832	2.9	5 1 2			2.1836	0.2	$\bar{6}$ 0 6			1.6225	0.1	14 0 4
		3.4268	0.1	$\bar{6}$ 1 1	2	2.153	2.1588	0.3	$\bar{7}$ 2 3			1.6133	0.1	$\bar{2}$ 2 8
		3.4066	0.1	6 1 1			2.1526	0.5	6 0 6			1.6077	0.3	2 2 8
		3.3654	0.2	$\bar{4}$ 1 3			2.1486	0.8	$\bar{8}$ 2 2			1.6046	0.1	$\overline{10}$ 1 7
7	**3.245**	3.2754	1.0	$\bar{4}$ 0 4			2.1433	0.2	$\overline{10}$ 1 3			1.5996	0.1	$\overline{12}$ 2 4
		3.2289	2.9	4 0 4			2.1403	0.2	$\bar{5}$ 1 6	3	1.5862	1.5940	0.2	$\overline{11}$ 2 5
		3.2153	0.7	1 1 4			2.1353	0.5	8 2 2			1.5832	0.3	12 2 4
		3.0623	0.1	$\bar{1}$ 2 1	2	2.113	2.1187	0.3	10 1 3			1.5755	0.2	11 2 5
		3.0598	0.3	1 2 1			2.1159	0.2	5 1 6			1.5748	1.1	0 4 0
1	3.000	3.0161	0.4	$\bar{1}$ 0 5			2.1104	0.4	$\bar{6}$ 2 4	2	1.5691	1.5688	0.2	$\overline{14}$ 2 0
		3.0046	0.3	1 0 5			2.1083	0.2	$\overline{11}$ 0 3			1.5651	0.4	$\overline{10}$ 2 6
8	**2.924**	2.9648	0.8	$\bar{7}$ 0 3	2	2.083	2.0916	0.5	6 2 4			1.5627	0.4	2 4 0
		2.9386	1.0	$\bar{8}$ 0 2			2.0903	0.1	$\overline{10}$ 0 4			1.5460	0.4	10 2 6
		2.9196	0.2	7 0 3			2.0881	0.2	$\overline{11}$ 1 2			1.5226	0.1	$\bar{6}$ 2 8
		2.9136	0.5	$\bar{7}$ 1 2			2.0822	0.8	$\bar{9}$ 2 1			1.5163	0.2	$\bar{9}$ 2 7
		2.9084	0.3	0 2 2			2.0754	0.5	9 2 1			1.4980	0.3	9 2 7
		2.9048	0.6	8 0 2			2.0714	0.2	11 1 2	2	1.4714	1.4702	0.1	$\bar{4}$ 3 7
		2.8996	1.9	$\bar{3}$ 2 1			2.0266	0.1	$\bar{2}$ 1 7			1.4693	0.3	$\overline{16}$ 0 4
		2.8934	1.4	3 2 1			2.0168	0.1	2 1 7			1.4664	0.2	$\bar{3}$ 2 9
		2.8848	0.4	7 1 2			1.9906	0.3	$\bar{8}$ 0 6	2	1.4536	1.4625	0.2	$\overline{13}$ 2 5
5	**2.869**	2.8683	0.9	$\bar{3}$ 0 5			1.9815	0.1	$\bar{7}$ 1 6			1.4593	0.2	3 2 9
		2.8630	0.4	6 1 3			1.9797	0.1	5 0 7			1.4568	0.2	$\overline{14}$ 2 4
		2.8388	1.1	3 0 5			1.9594	0.2	8 0 6			1.4524	0.2	16 0 4
												1.4456	0.1	13 2 5

Table 3. Data collection and structure refinement details for ferraioloite.

Diffractometer	ADSC Quantum 315r detector
X-ray radiation/power	λ = 0.7100 Å
Temperature	100 K
Structural formula	$MgMn^{2+}{}_4(Fe^{2+}{}_{0.5}Al^{3+}{}_{0.5})_4$ $Zn_4(PO_4)_8(OH)_4(H_2O)_{20}$
Space group	*I*2/*m*
Unit-cell dimensions	*a* = 25.333(3) Å *b* = 6.299(1) Å *c* = 15.161(3) Å β = 90.93(3)°
V	2419.0(2) Å^3
Z	2
Absorption coefficient	3.978 mm^{-1}
F(000)	1717
Crystal size	20 × 10 × 2 μm
θ range	1.55 to 30.52°
Index ranges	$-36 \leq h \leq 35$, $-7 \leq k \leq 7$, $-21 \leq l \leq 21$
Reflections collected/unique	17759/751 [R_{int} = 0.1455]
Reflections with [$I > 3\sigma(I)$]	565
Refinement method	Full-matrix least-squares on F^2
Parameters refined	98
Final *R* indices [$I > 3\sigma(I)$]	R_{obs} = 0.065, wR_{obs} = 0.071
R indices (all data)	R_{obs} = 0.092, wR_{obs} = 0.0773
Extinction coefficient	0.0006(11)
delta*F*, min, max	−0.70, 0.49

the micro-focus macromolecular beam line MX2 of the Australian Synchrotron. Data were collected at 100 K using an ADSC Quantum 315r detector and monochromatic radiation with a wavelength of 0.71086 Å. A φ scan was employed, with frame widths of 1° and a counting time per frame of 1 s. The data was integrated in *P*1 using XDS (Kabsch, 2010) and the absorption correction was carried out with SADABS (Bruker, 2001). The ultra-thin laths of ferraioloite gave relatively poor diffraction, with severe streaking of the diffraction spots and it was necessary to restrict the data used in the analysis to a resolution of 1 Å. Indexing of the synchrotron data gave a near-orthogonal body-centred cell with *a* = 25.333, *b* = 6.299, *c* = 15.161 Å, α = 90.47, β = 90.93 and γ = 89.91°. The departure of α and γ from 90° was considered to be due to problems with centring on the streaked reflections. A structure solution was obtained in the monoclinic space group *I*2/*m* using SHELXT (Sheldrick, 2008, 2015). The close similarity of the heteropolyhedral layer model obtained to that for falsterite (Kampf *et al.*, 2012) assisted in the assignment of cations to the different metal atom sites. As the refinement progressed, it became evident from site occupancies and bond distances that the Ca site in falsterite was replaced by Mn and the Fe sites, which contain $0.5Fe^{2+}$+$0.5Fe^{3+}$ in falsterite, have the Fe^{3+} replaced by Al^{3+} in ferraioloite. The structure was refined using JANA2006 (Petříček & Dušek, 2006).

Table 4. Atom fractional coordinates, isotropic displacement parameters (Å^2) and site occupancies for ferraioloite.

	x	*y*	*z*	U_{iso}	Occ.	Bond valence
Heteropolyhedral layer atoms						
Zn	0.3138(7)	0.7478(2)	0.5013(1)	0.0408(8)	1	2.15
Mn1	0.1678(1)	0.5	0.6201(2)	0.042(1)	1	1.59
Mn2	0.1667(1)	0	0.3754(2)	0.044(1)	1	1.76
Fe1	0.25	0.25	0.75	0.042(2)	0.66(2)	2.65
Al1	0.25	0.25	0.75	0.042(2)	0.34(2)	
Fe2	0.75	0.25	0.75	0.053(2)	0.46(3)	2.59
Al2	0.75	0.25	0.75	0.053(2)	0.54(3)	
P1	0.2201(2)	0.5	0.4276(3)	0.042(2)	1	5.00
P2	0.3519(2)	0	0.3405(3)	0.036(1)	1	4.84
P3	0.2212(2)	0	0.5766(3)	0.033(1)	1	5.01
P4	0.3512(2)	0.5	0.6655(4)	0.046(2)	1	4.90
O1	0.2204(3)	0.3096(11)	0.3655(5)	0.026(2)	1	1.77
O2	0.2709(3)	0.5	0.4868(5)	0.005(2)	1	2.33
O3	0.1703(4)	0.5	0.4836(9)	0.053(4)	1	1.71
O4	0.3886(5)	0	0.2608(7)	0.046(4)	1	1.25
O5	0.2958(4)	0	0.2987(8)	0.025(3)	1	1.60
O6	0.3580(3)	0.1957(11)	0.4021(5)	0.028(2)	1	1.74
O7	0.2205(3)	0.2034(12)	0.6310(5)	0.031(2)	1	1.92
O8	0.2691(5)	0	0.5149(9)	0.057(4)	1	2.22
O9	0.1746(7)	0	0.510(1)	0.120(8)	1	1.69
O10	0.3587(3)	0.6956(11)	0.6062(5)	0.030(2)	1	1.73
O11	0.3944(4)	0.5	0.7387(6)	0.020(3)	1	1.22
O12	0.2977(5)	0.5	0.7129(10)	0.062(5)	1	1.79
O13 (OH)	0.2961(5)	0	0.7378(9)	0.036(3)	1	0.95
O14 (OH)	0.2018(10)	0	0.249(2)	0.109(7)	1	0.86
O15 (H_2O)	0.1018(6)	0.754(2)	0.390(1)	0.092(5)	1	0.25
O16 (H_2O)	0.0934(7)	0.289(3)	0.636(1)	0.102(5)	1	0.23
Interlayer atoms						
Mg	0.5	0.5	0.5	0.056(3)	1	2.66
Ow1*	0.505(1)	0	0.327(2)	0.119(8)	1	0.1
Ow2	0.5629(5)	0.5	0.5975(8)	0.034(3)	1	0.29
Ow3	0.5113(9)	0.5	0.749(2)	0.101(7)	1	0.1
Ow4	0.5279(7)	0.746(2)	0.440(1)	0.103(5)	1	0.52
Ow5	0.5	0.252(5)	0	0.16(1)	1	0.1

*Ow = interlayer water molecules

Refinement employing isotropic displacement parameters converged at R_{obs} = 0.07 for 751 reflections at a resolution of 1.0 Å. Details of the data collection and structure refinement are provided in Table 3. Fractional coordinates, site occupancies and isotropic atom displacement parameters are given in Table 4. Included in Table 4 are bond valences calculated in JANA2006. Selected bond distances are reported in Table 5.

6. Discussion of structure

The structure of ferraioloite is shown in projection along [010] in Fig. 3a. It is a heteropolyhedral layer structure with layers parallel to (100) and with isolated $Mg(H_2O)_6$ octahedra and water molecules packing between the layers. The heteropolyhedral slabs have the same topology as those in the mineral falsterite, $Ca_2MgMn^{2+}{}_2(Fe^{2+}{}_{0.5}Fe^{3+}{}_{0.5})_4Zn_4(PO_4)_8(OH)_4(H_2O)_{14}$ (Kampf *et al.*, 2012), shown in Fig. 3b, with Mn^{2+} replacing Ca^{2+} and with Al^{3+} substituting for Fe^{3+}. In falsterite, the slabs are bridged by edge-sharing dimers of MgO_6 octahedra which share edges with ZnO_4 tetrahedra in adjacent slabs. The Mg sites are half occupied in falsterite. In contrast, ferraioloite has isolated, fully occupied $Mg(H_2O)_6$ octahedra between the slabs, and cohesion is maintained by hydrogen bonding between the water molecules and oxygen acceptors in the slabs as shown by the dashed lines in Fig. 3a. The replacement of the bridging dimeric units with H-bonded $Mg(H_2O)_6$ octahedra results in a large (19%) expansion of the axis, normal to the layers, from 21.3 Å in falsterite to 25.3 Å in ferraioloite.

The H atoms were not located in the structure refinement, but the assignment of OH^- and H_2O can be inferred from bond-valence calculations, the results of which are

Table 5. Selected bond distances (Å) in ferraioloite.

Zn	O10	1.967(9)	Fe2	O1	1.953(8)
	O2	1.913(5)		O1	1.953(8)
	O8	1.963(7)		O5	2.084(6)
	O6	1.923(8)		O5	2.084(6)
	<Zn-O>	1.942		O14	1.99(2)
				O14	1.99(2)
Mn1	O13	2.333(14)		<Fe-O>	2.009
	O7	2.308(8)			
	O7	2.308(8)	P1	O1	1.525(8)
	O3	2.072(13)		O1	1.525(8)
	O16	2.311(17)		O2	1.556(9)
	O16	2.311(17)		O3	1.533(13)
	<Mn-O>	2.273		<P-O>	1.535
Mn2	O1	2.384(8)	P2	O4	1.536(13)
	O1	2.384(8)		O5	1.547(11)
	O14	2.10(3)		O6	1.553(8)
	O14	2.04(2)		O6	1.553(8)
	O15	2.27(1)		<P-O>	1.547
	O15	2.27(1)			
	<Mn-O>	2.241	P3	O7	1.524(8)
				O7	1.524(8)
Mg	Ow2	2.156(12)		O8	1.544(14)
	Ow2	2.156(12)		O9	1.54(2)
	Ow4	1.934(15)		<P-O>	1.533
	Ow4	1.934(15)			
	Ow4	1.934(15)	P4	O10	1.538(8)
	Ow4	1.934(15)		O10	1.538(8)
	<Mg-O>	2.008		O11	1.544(10)
				O12	1.545(13)
Fe1	O13	1.971(8)		<P-O>	1.541
	O13	1.971(8)			
	O7	1.965(8)			
	O7	1.965(8)			
	O12	2.068(8)			
	O12	2.068(8)			
	<Fe-O>	2.001			

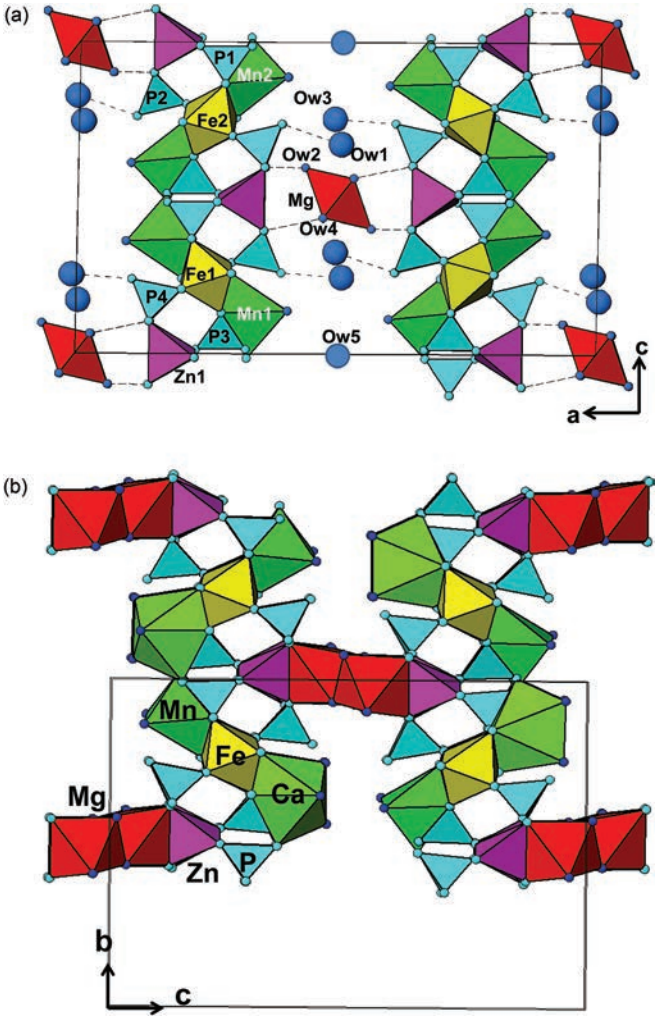

Fig. 3. (a) Crystal structure of ferraioloite. Dashed lines correspond to hydrogen bonds between interlayer water molecules and layer oxygen atoms. (b) Crystal structure of falsterite. (online version in colour)

Table 6. Comparative data for ferraioloite and falsterite.

	Ferraioloite	Falsterite
Formula	$MgMn^{2+}{}_4(Fe^{2+}{}_{0.5}Al^{3+}{}_{0.5})_4Zn_4(PO_4)_8(OH)_4(H_2O)_{20}$	$Ca_2MgMn^{2+}{}_2(Fe^{2+}{}_{0.5}Fe^{3+}{}_{0.5})_4Zn_4(PO_4)_8(OH)_4(H_2O)_{14}$
Symmetry	Monoclinic, *I*2/m	Monoclinic, $P2_1/c$
Cell	*a* = 25.333(3) Å, *b* = 6.299(1) Å, *c* = 15.161(3) Å, β = 90.93(3)°	*a* = 6.387(2) Å, *b* = 21.260(7) Å, *c* = 15.365(5) Å, *β* = 90.564(6)°
	V = 2419.0(2) Å^3	*V* = 2086.2(1.1) Å^3
Z	2	2
Strongest powder-pattern lines *d, I, hkl*	12.7, 100 (200)	12.86, 34 (011)
	4.78, 4 (112)	10.675, 100 (020)
	3.499, 5 ($\bar{5}$12)	4.043, 18 ($\bar{1}$32)
	3.245, 7 (404)	3.220, 25 ($\bar{1}$52)
	2.924, 8 ($\bar{3}$21)	3.107, 14 (044)
	2.869, 5 (305)	2.846, 19 ($\bar{2}$22)
Optics	Biaxial (−)	Biaxial (-)
	α = 1.575(calc), *β* = 1.5825(5), *γ* = 1.5835(5)	*α* = 1.575(10), *β* = 1.600(5), *γ* = 1.610(5)
	2*V*(meas.) = 40(5)°; 2*V*(calc.) = 40°	2*V*(meas.) = 60(10)°; 2*V*(calc.) = 63.8°
	Pleochroism: *X*, *Z* = colourless,	Pleochroism: *X*, *Z* = colourless to very pale yellow,
	Y = blue grey; *Y* >> *X* ≈ *Z*	*Y* = blue green; *Y* >> *X* ≈ *Z*
	Orientation: *X* ≈ **a**, *Y* = **b**, *Z* ≈ **c**	Orientation: *X* ≈ **b**, *Y* = **a**, *Z* ≈ **c**

given in Table 4. These show that the anions forming shared edges between the Mn-centred and Fe-centred octahedra, O13 and O14, are hydroxyl ions, and the unshared vertices of the Mn-centred octahedra, O15 and O16, are water molecules. The unshared vertices O4 and O11 of the P2- and P4-centred tetrahedra have low valence sums, 1.25 and 1.22, respectively. The valence requirements for these oxygen atoms are met by H-bonding as shown in Fig. 3a. The sites Fe1 and Fe2 contain a mixture of Al and Fe, and the valence sums for these sites, 2.65 and 2.59, respectively, are consistent with the Fe being predominantly in the divalent state. This compares with falsterite, where these two sites contain an equal mixture of Fe^{2+} and Fe^{3+}. Ferraioloite is closely related to falsterite, both structurally and chemically. A comparison of the properties of the two minerals is given in Table 6.

The pleochroic colours exhibited by ferraioloite and falsterite deserve additional comment. Both minerals exhibit distinct colour only along their 6-Å axis, **b** in ferraioloite and **a** in falsterite. This is the direction of edge-sharing chains of Fe1 and Fe2 octahedra in each structure. Falsterite exhibits a strong blue-green colour in this direction, while ferraioloite exhibits a distinctly less intense blue-grey colour. Kampf *et al.* (2012) attributed the colour in falsterite to the strong absorption typical of $Fe^{2+}-Fe^{3+}$ charge transfer. It seems likely that the blue-grey colour observed for ferraioloite is also due to $Fe^{2+}-Fe^{3+}$ charge transfer along this chain and that it is much weaker because only a very small portion of the Fe is trivalent and the presence of Al^{3+} effectively ''dilutes'' the effect of the charge transfer.

Acknowledgements: Two anonymous referees are thanked for their helpful comments on the manuscript. Part of this study was funded by the John Jago Trelawney Endowment to the Mineral Sciences Department of the Natural History Museum of Los Angeles County.

References

Atencio, D., Matioli, P.A., Smith, J.B., Chukanov, N.V., Coutinho, J.M.V., Rastsvetaeva, R.K., Möckel, S. (2008): Footemineite, the Mn-analog of atencioite, from the Foote mine, Kings Mountain, Cleveland County, North Carolina, U.S.A., and its relationship with other roscherite-group minerals. *Am. Mineral.*, **93**, 1–6.

Bruker (2001): *SAINT* Version 6.02 (includes *XPREP* and *SADABS*). Bruker AXS Inc, Madison, Wisconsin, USA.

Ferraiolo, J.A. (1982): A systematic classification of nonsilicate minerals. *Bull. AMNH*, **172**, article 1.

Ferraiolo, J.A. (2012): Ferrolaueite - new occurrences. *Austral. J. Mineral.*, **16**, 77–78.

Kabsch, W. (2010): XDS. *Acta Crystallogr.*, **D66**, 125–132.

Kampf, A.R. (1977): Schoonerite: its atomic arrangement. *Am. Mineral.*, **62**, 250–255.

Kampf, A.R., Mills, S.J., Simmons, W.B., Nizamoff, J.W., Whitmore, R.W. (2012): Falsterite, $Ca_2MgMn^{2+}{}_2Fe^{2+}{}_2Fe^{3+}{}_2Zn_4(PO_4)_8(OH)_4(H_2O)_{14}$, a new secondary phosphate mineral from the Palermo No. 1 pegmatite, North Groton, New Hampshire. *Am. Mineral.*, **97**, 496–502.

Moore, P.B. & Kampf, A.R. (1977): Schoonerite, a new zinc-manganese-iron phosphate mineral. *Am. Mineral.*, **62**, 246–249.

Petříček, V., & Dušek, M. (2006): *JANA2006. Structure Determinations Software Programs*. Institute of Physics, Academy of Sciences of the Czech Republic, Prague.

Segeler, C.G., Moore, P.B., Dyar, M.D., Leans, F., Ferraiolo, J.A. (2012): Ferrolaueite, a new mineral from Monmouth County, New Jersey, USA. *Austral. J. Mineral.*, **16**, 69–76.

Sheldrick, G.M. (2008): A short history of SHELX. *Acta Crystallogr.*, **A64**, 112–122.

Sheldrick, G.M. (2015): SHELXT-Integrated space-group and crystal-structure determination. *Acta Crystallogr.*, **A71**, 3–8.

White, J.S. (1981): Mineralogy of the Foote Mine, Kings Mountain, North Carolina. *Carol. Geol. Soc. Fld. Trip Guidebk.*, 39–48.

Received 19 November 2015
Modified version received 14 January 2016
Accepted 15 January 2016